

LUCY Y. PAO
and KATHRYN E. JOHNSON

Control of Wind Turbines

APPROACHES, CHALLENGES, AND RECENT DEVELOPMENTS

Wind energy is a fast-growing interdisciplinary field that encompasses multiple branches of engineering and science. According to the World Wind Energy Association, the global installed capacity of wind turbines grew at an average rate of 27% per year over the years 2005–2009 [1]. At the end of 2009, the installed capacity in the United States was about 35,000 MW [2], while the worldwide installed capacity was approximately 160,000 MW (see Figure 1). Wind is recognized worldwide as a cost-effective, environmentally friendly solution to energy shortages. Although the United States receives only about 2% of its electrical energy from wind [2], that figure in Denmark is approximately 20% [3]. The comprehensive report [4] by the U.S. Department of Energy lays the framework for achieving 20% of the U.S. electrical energy generation from wind by the year 2030. This report covers technological, manufacturing, transmission and integration, market, environmental, and siting factors.

Despite the growth in the installed capacity of wind turbines in recent years, engineering and science challenges remain. Because larger wind turbines have energy-capture and economic advantages, the typical size of utility-scale wind turbines has grown by two orders of magnitude over the last three decades (see Figure 2). Since modern wind turbines are large, flexible structures operating in uncertain environments, advanced control technology can improve their performance. For example, advanced controllers can help decrease the cost of wind energy by increasing turbine efficiency, and thus energy capture, and by reducing structural loading, which increases the lifetimes of the

PHOTO BY L. FINGERSH

Digital Object Identifier 10.1109/MCS.2010.939962

Date of publication: 16 March 2011

components and structures. The goal of this tutorial is to describe the technical challenges in the wind industry relating to control engineering.

Although a wind turbine can be built in either a vertical-axis or horizontal-axis configuration, as shown in Figure 3, we focus on horizontal-axis wind turbines (HAWTs) because they dominate the utility-scale wind turbine market. At the utility scale, HAWTs have aerodynamic and practical advantages [5], [6]. Smaller vertical axis wind turbines (VAWTs) are more likely to use passive rather than active control strategies. The generating capacity of commercially available HAWTs ranges from less than 1 kW to several megawatts. Active control is more cost effective on larger wind turbines than smaller ones, and therefore this tutorial focuses on HAWTs whose capacity is 600 kW or larger.

The next section describes the configurations and basic operation of wind turbines. We then explain the layout of a wind turbine control system by taking a “walk” around the wind turbine control loop, with discussions on wind inflow characteristics, available sensors and actuators, and turbine modeling for use in control. Subsequently, we describe the current state of wind turbine control, which is followed by a discussion of the issues and opportunities in wind turbine and wind farm control. At the end, we give some concluding remarks.

WIND TURBINE BASICS

The main components of a HAWT that are visible from the ground are the tower, nacelle, and rotor, as shown in Figure 4. The airfoil-shaped blades capture the kinetic energy of the wind and transform it into the rotational kinetic energy of the wind turbine’s rotor. The rotor drives the low-speed shaft, which in turn drives the gearbox. The gearbox steps up the rotational speed and drives the generator by means of the high-speed shaft. The gearbox, high-speed shaft, and generator are housed in the nacelle, along with part of the low-speed shaft. Direct drive configurations without gearboxes are being developed to eliminate costly gearbox failures.

Wind turbines may be variable or fixed speed. Variable-speed turbines tend to operate closer to their maximum aerodynamic efficiency for a higher fraction of the time but require electrical power processing so that the generated electricity can be fed into the electrical grid at the proper frequency. Variable-speed turbines are more cost effective and thus more popular than constant-speed turbines at the utility scale because of improvements in generator and power electronics technologies. Variable-speed operation can also reduce turbine loads, since sudden increases in wind energy due to gusts can be absorbed by an increase in rotor speed rather than by component bending.

The goals and strategies of wind turbine control are affected by the turbine configuration. A HAWT can be upwind, with the rotor on the upwind side of the tower, or

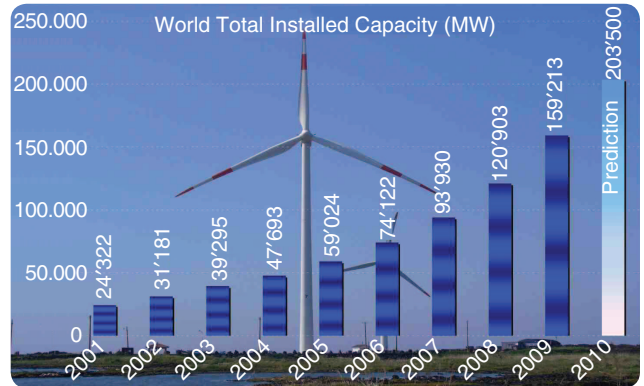


FIGURE 1 Installed wind energy capacity worldwide. Projected growth in worldwide capacity is driving the need for advances in wind science and engineering, including advanced control techniques. (Reproduced with permission from [1].)

downwind, with the rotor on the downwind side of the tower. This choice affects the turbine dynamics and thus the structural design. A wind turbine can also be variable pitch or fixed pitch, meaning that the blades may or may not be able to rotate about their longitudinal axes. Variable-pitch turbines might allow all or part of their blades to rotate along the pitch axis. Fixed-pitch machines are less expensive to build, but the ability of variable-pitch turbines to mitigate loads and affect the aerodynamic torque has driven their dominance in modern utility-scale turbine markets.

The example given in Figure 5 shows power curves for a 2.5-MW variable-speed turbine and a 2.5-MW fixed-speed

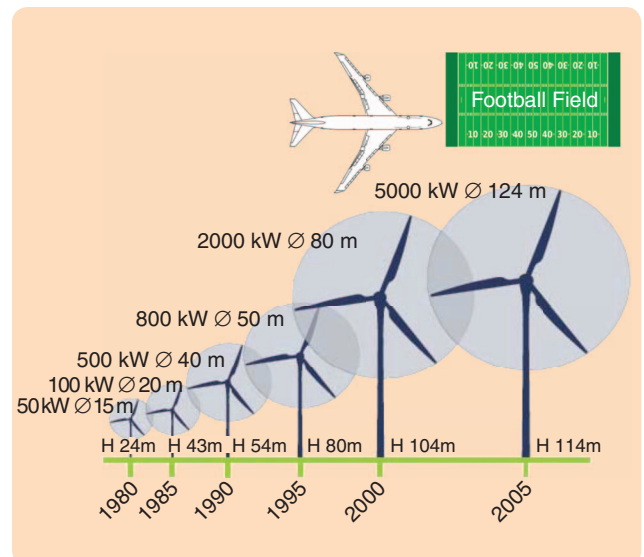


FIGURE 2 Utility-scale wind turbines shown with schematics of a Boeing 747 and an American football field on the same scale. Advanced control methods can be used to improve wind turbine power, energy capture, and power quality while reducing structural loading, which decreases maintenance requirements and extends lifetime. This diagram shows the progression of ever larger commercial turbines over the last three decades. (Diagram and schematics used with permission from [45]–[47].)



(a)



(b)

FIGURE 3 Vertical-axis and horizontal-axis wind turbines. (a) A vertical-axis turbine spins like a top and does not need to be yawed into the wind. Its heavy components, such as the generator and gearbox, can be located on the ground. (Photo from [48].) (b) Horizontal-axis turbines placed on tall towers can catch the faster wind higher above the ground. [Figure (b) courtesy of Lee Jay Fingersh of the U.S. National Renewable Energy Laboratory (NREL).]

turbine, as well as a curve showing the available wind power for a turbine with the same rotor size as these two turbines. For both turbines, when the wind speed is low, the power available in the wind is low compared to losses in the turbine system; hence, the turbines are not run. This operational region is known as Region 1. When the wind speed is above the rated wind speed, corresponding to Region 3,

power is limited for both turbines to avoid exceeding safe electrical and mechanical load limits. In this example, low wind speed is considered to be below 6 m/s, whereas high wind speed is above the rated wind speed of 11.7 m/s.

The main difference in the example shown in Figure 5 between the two types of turbines appears for mid-range wind speeds, corresponding to Region 2, which encompasses

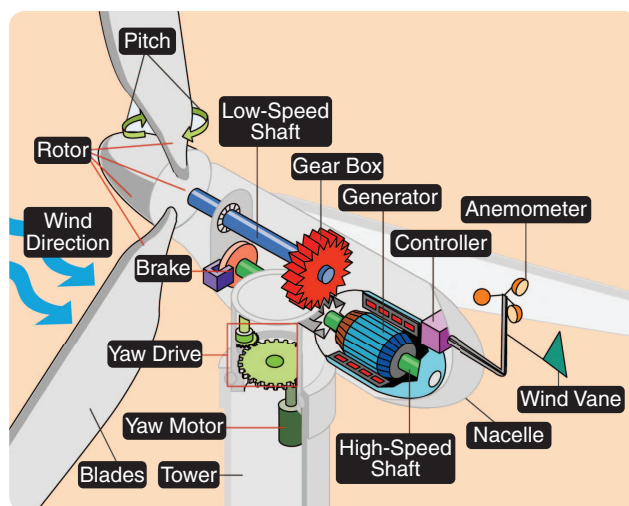


FIGURE 4 Wind turbine components. The wind first encounters the rotor on this upwind horizontal-axis turbine, causing it to spin. The low-speed shaft transfers energy to the gearbox, which steps up in speed and spins the high-speed shaft. The high-speed shaft causes the generator to spin, producing electricity. Also shown is the yaw-actuation mechanism, which is used to turn the nacelle so that the rotor faces into the wind. (Figure courtesy of the U.S. Department of Energy [49].)

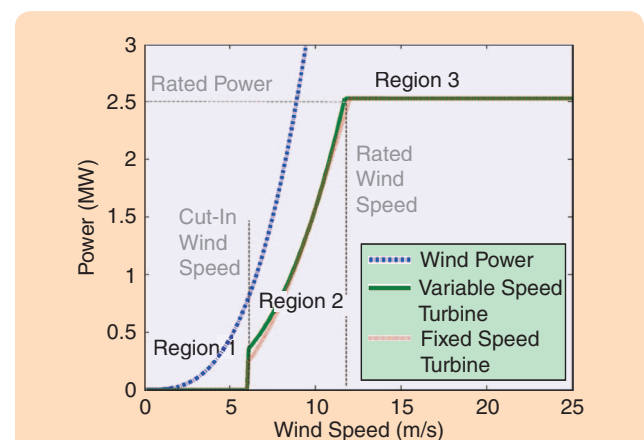


FIGURE 5 Illustrative power curves. The wind power curve shows the power available in the wind for the example variable- and fixed-speed turbines with the same rotor diameter. The turbines are started up at 6 m/s wind speed when there is enough wind to overcome losses and produce power. Above 11.7 m/s wind speed, power is limited to protect the turbines' electrical and mechanical components. Both turbines generate the same power at the fixed-speed turbine's 10 m/s design point, but the variable speed turbine generates more power at all wind speeds in Region 2, with a maximum difference of about 150 kW at 6 m/s.

The increasing dimensions of wind turbines lead to the increase in the loads on wind turbine structures.

wind speeds between 6 and 11.7 m/s. Except for the fixed-speed turbine's design operating point of 10 m/s, the variable-speed turbine in Figure 5 converts more power at each wind speed than the fixed-speed turbine. This example illustrates the fact that variable-speed turbines can operate at maximum aerodynamic efficiency over a wider range of wind speeds than fixed-speed turbines.

The maximum difference between the two curves in Region 2 is 150 kW. The wind speed probability distribution can be modeled as a Weibull function, with scale and shape parameters that define the function [5], [6]. In the case of a Weibull distribution having a shape parameter $k = 2$ and scale parameter $c = 8.5$, the variable-speed turbine captures 2.3% more energy per year than the constant-speed turbine. A wind farm rated at 100 MW and operating with a 35% capacity factor can produce about 307 GWh of energy in a given year. If the cost of energy is US\$0.04 per kilowatthour, each gigawatthour is worth about US\$40,000, and each 1% loss of energy on this wind farm is equivalent to a loss of US\$123,000 per year [7].

Not shown in Figure 5 is the high wind cut-out, the wind speed above which the turbine is powered down and stopped to avoid excessive operating loads. High wind cut-out typically occurs at wind speeds between 20 and 30 m/s for utility-scale turbines.

Momentum theory using an actuator disc model of a wind turbine rotor shows that the maximum aerodynamic efficiency, called the Betz limit [5], [8], is approximately 59% of the wind power. The aerodynamic efficiency, which is the ratio of the turbine power to the wind power, is given by the power coefficient

$$C_p = \frac{P}{P_{\text{wind}}}, \quad (1)$$

where P is the instantaneous turbine power and

$$P_{\text{wind}} = \frac{1}{2} \rho A v^3 \quad (2)$$

is the instantaneous power available in the wind for a turbine of that rotor diameter. In (2), ρ is the air density, A is the swept area πR^2 of the rotor, R is the rotor radius, and v is the instantaneous wind speed, which is assumed to be uniform across the rotor swept area. The swept area is the area of the disk circumscribed by the blade tip.

Finally, utility-scale wind turbines are either two or three bladed. Two-bladed turbines typically use a teetering hinge to allow the rotor to respond to differential loads [6], [9]. This teeter hinge allows one blade to move upwind

while the other moves downwind in response to differential wind loads, much like a seesaw allows one child to move up while another moves down. For a turbine with an even number of blades placed symmetrically around the rotor, when one blade is at the uppermost position, another blade is in the slower wind caused by either the tower shadow behind the tower or the bow wake in front of the tower. This discrepancy is exacerbated by typical wind shear conditions, which result in higher wind speeds higher above the ground. Three-bladed turbines tend to experience more symmetrical loading than two-bladed turbines, but at a 50% increase in blade cost [5], [6].

A WALK AROUND THE WIND TURBINE CONTROL LOOPS

In designing controllers for wind turbines, it is often assumed as in (2) that the wind speed is uniform across the rotor plane. However, as shown by the instantaneous wind field in Figure 6, the wind input may vary in space and time over the rotor plane. The deviations of the wind speed from the nominal wind speed across the rotor plane can be considered disturbances for control design.

Utility-scale wind turbines have several levels of control, namely, supervisory, operational, and subsystem. As shown in Figure 7, the top-level supervisory control determines when the turbine starts and stops in response to changes in the wind speed and also monitors the health of the turbine. The operational control determines how the turbine achieves its control objectives in Regions 2 and 3. The subsystem controllers are responsible for the generator, power electronics, yaw drive, pitch drive, and remaining actuators. In this section, we move through the operational control loops shown in Figure 6, describing the wind inflow, sensors, actuators, and turbine model while treating the subsystem controllers as black boxes. The pitch and torque controllers in Figure 6 are discussed in the section "Feedback Control." The details of the subsystem controllers are beyond the scope of this article; see [5] and [6].

Wind Inflow

The differential heating of the Earth's atmosphere is the driving mechanism for the wind. Various atmospheric phenomena, such as the nocturnal low-level jet, sea breezes, frontal passages, and mountain and valley flows, affect the wind inflow across a wind turbine's rotor plane [5], which spans from 60 m to 180 m above the ground for megawatt utility-scale wind turbines, as

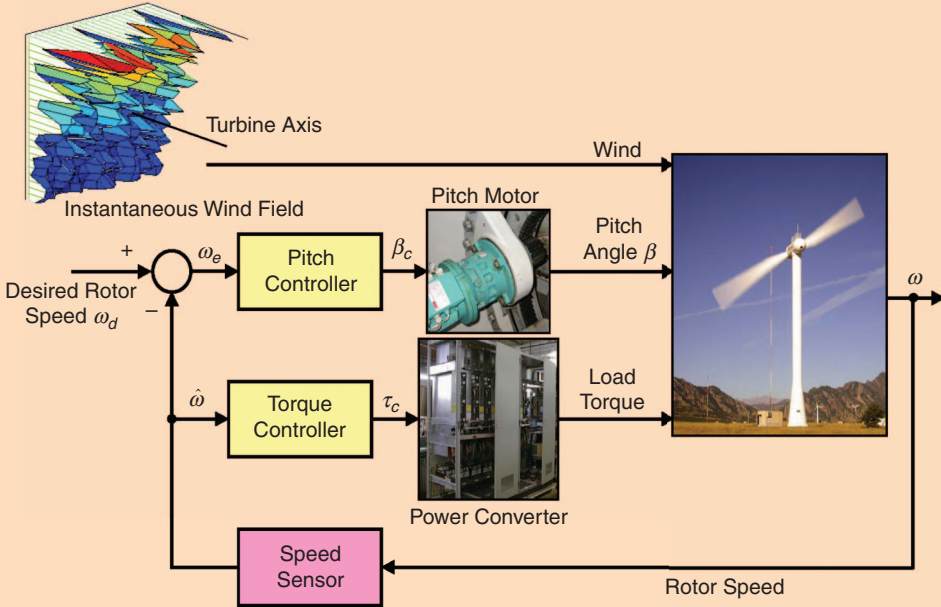


FIGURE 6 Wind turbine control feedback loops. Since the wind speed varies across the rotor plane, wind speed point measurements convey only a small part of the information about the wind inflow. Rotor speed is the only measurement required for the baseline generator torque and blade-pitch controllers described in this article.

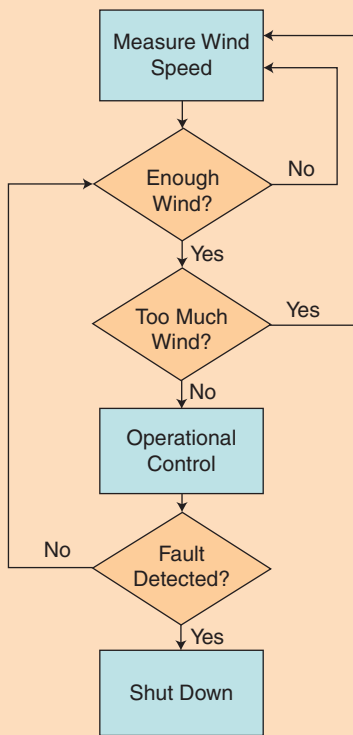


FIGURE 7 Wind turbine supervisory control logic. If the wind conditions are right to run the turbine, the operational controller sends appropriate signals to the yaw drive, blade-pitch actuators, and generator torque actuator. The supervisory controller continues to monitor for faults and shuts down the turbine if a fault is detected.

shown in Figure 2. Given the large rotor plane and the variability of the wind, hundreds of sensors would be required to characterize the spatial variation of the wind speed encountering the entire span of each blade.

The available wind resource can be characterized by the spatial or temporal average of the wind speed; the frequency distribution of wind speeds; the temporal and spatial variation in wind speed; the most frequent wind direction, also known as the prevailing wind direction; and the frequency of the remaining wind directions [5]. The probability of the wind speed being above a given turbine's rated wind speed can be used to predict how often the turbine operates in Region 3 at its maximum, that is, rated, power generation capacity. The capacity factor CF is defined by the ratio

$$CF = \frac{E_{\text{out}}}{E_{\text{cap}}}, \quad (3)$$

where E_{out} is a wind turbine's energy output over a period of time and E_{cap} is the energy the turbine would have produced if it had run at rated power for the same amount of time. Capacity factor can also describe the fraction of available energy captured by N turbines in a wind farm.

To predict the capacity factor and maintenance requirements for a wind turbine, it is useful to understand wind characteristics over both long and short time scales, ranging from multiyear to subsecond. Determining whether a location is suitable and economically advantageous for siting a wind turbine depends on the ability to measure and predict the available wind resource at that site. Significant variations

in seasonal average wind speeds affect a local area's available wind resource over the course of each year. Wind speed and direction variations caused by the differential heating of the Earth's surface during the daily solar radiation cycle occur on a diurnal, that is, daily time scale. The ability to predict hourly wind speed variations can help utilities to plan their energy resource portfolio mix of wind energy and additional sources of energy. Finally, knowledge of short-term wind speed variations, such as gusts and turbulence, is used in both turbine and control design processes so that structural loading can be mitigated during these events.

Since wind inflow characteristics vary temporally and spatially across the turbine's rotor plane, assuming uniform constant wind across the rotor plane is problematic for control design for large rotor sizes. The uniform wind assumption, which is used in (1) and (2), can lead to poor predictions of the available wind power and loading on the turbine. Especially problematic are nonuniform winds such as low-level jets [10]. Analysis indicates that rotor-sized or smaller (see Figure 2) turbulent structures in the wind can cause more damage than turbulent structures that are larger than the rotor [11]–[13].

Improved capabilities for measuring and predicting turbulent events are needed [14], and this area of research is active among atmospheric scientists [15]–[17]. Figure 8 shows measurements of coherent turbulent kinetic energy in a low-level jet, a frequent atmospheric feature in some parts of the United States. Significant energetic structures are located between 40 and 120 m above ground level, within the typical height range for a utility-scale turbine rotor. Controllers designed to alleviate structural loading in response to turbulent structures are described in [12] and [18].

Sensors

As shown in Figure 6, the rotor speed measurement is used in feedback for basic control in both Regions 2 and 3. Since the gearbox ratio is known, the rotor speed can be measured on either the high- or low-speed shaft. Rotor-speed measurements can be used for speed and power control but might not be suitable for more sophisticated control objectives, such as reducing torsional oscillations in the drivetrain.

In addition to rotor-speed measurements, anemometers are used for supervisory control, in particular to determine whether the wind speed is sufficient to start turbine operation. Figure 9 shows sonic and propeller anemometers on a meteorological tower. For measuring wind speed and wind direction, the majority of turbines have an anemometer and wind vane located on top of the nacelle at approximately the hub height. Because of the interaction between the rotor and the wind, the measurements are distorted in both upwind and downwind turbines.

Power measurement devices are used to assess energy generation. Additional sensors that are sometimes found on wind turbines include strain gages on the tower and

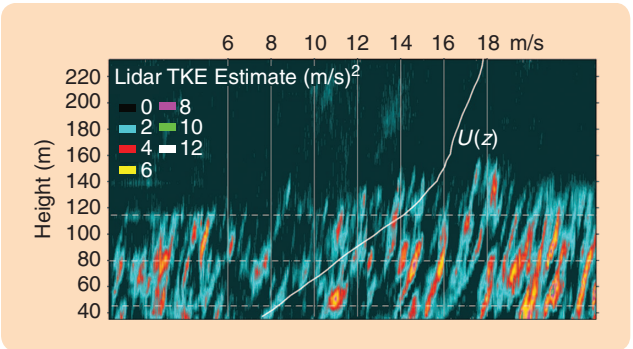


FIGURE 8 High-resolution Doppler lidar measurements showing coherent turbulent kinetic energy (TKE). Coherent TKE can cause excessive loading on a wind turbine. The majority of the TKE occurs between 40–120 m, which is a typical range for a utility-scale turbine rotor. (Reproduced with permission from [50].)

blades, accelerometers, position encoders on the drive shaft and blade-pitch actuation systems, and torque transducers [5], [6].

Sensors used for control, especially rotor or generator speed sensors and wind vanes, must be reliable. Fault detection can be used to identify faulty sensors [19], [20], and practical problems related to the size of turbines and their noisy environments can hinder sensor failure diagnoses [21]. Calibration drift is a typical failure mode, especially for strain gages and accelerometers, and thus controllers that depend on sensors prone to drift must be robust to calibration errors such as unknown biases.

Actuators

Utility-scale wind turbines typically have up to three main types of actuators. A yaw motor, which aligns the nacelle

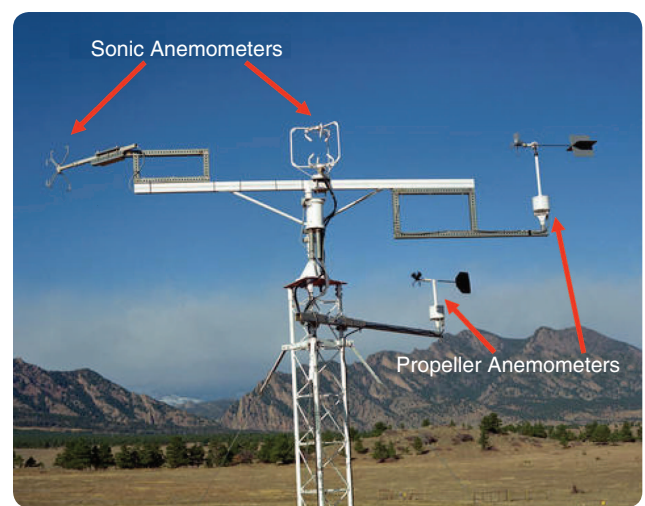


FIGURE 9 Several types of sonic and propeller anemometers on a meteorological tower at NREL's National Wind Technology Center near Boulder, Colorado. Unlike anemometers placed on a meteorological tower for a research turbine, nacelle-mounted anemometers on commercial wind turbines experience wind speed disruption from the rotor. (Photo courtesy of NREL, picture number 00215, taken by Warren Gretz.)

Advanced Control of Wind Turbines

Advanced controllers that go beyond the baseline can improve wind turbine performance. In 2009 and 2010, the number of publications describing advanced wind turbine control strategies rose dramatically compared to previous years. We mention a subset of these publications, which encompass a wide range of control structures over a set of desired objectives. All are ultimately driven by the goal of reducing the cost of wind energy, either by reducing cost, increasing energy capture, or some combination thereof.

LOAD REDUCTION

Cost reduction can be achieved by means of load reduction, which can either reduce maintenance costs over a turbine's lifespan or allow the turbine to be built in a less expensive manner initially. Early controllers used individual pitch control to reduce component loads [S1], [S2].

Disturbance accommodating control (DAC) for reducing turbine loads is considered in [12], [33], and [S3]–[S5]. DAC was originally developed as a model-based state-space technique to mitigate the effect of persistent disturbances [S6]. Disturbance tracking control is a variation of DAC also used in wind turbine control [S3]. As shown in Figure S1, DAC models and estimates disturbances within the control loop. DAC uses functional models of disturbances rather than statistical descriptions that are common with random noise disturbances. The periodic once-per-revolution disturbances due to wind shear [33] and hydrodynamic wave disturbances that affect offshore turbines [S4] can be modeled using a sum of sinusoidal functions with known frequencies. The disturbance

estimate enables a separate estimate of the wind turbine state to be obtained, and the turbine state estimate is then used to compute the control input to the wind turbine. Since DAC affects only the state observer, the wind turbine control design need not be changed with the decision to use DAC.

Alternative control techniques for reducing loads are considered in [S7]–[S10]. In [S7], a linear parameter-varying (LPV) controller with wind speed estimation is shown in simulation to reduce damage at low, medium, and high wind speeds with little reduction in energy capture. In [S8], the feedback linearized controller with extended Kalman filter regulates speed, power, and drivetrain torsion with mixed results. Passive and active structural control techniques studied in the area of earthquake engineering and building control systems are also being investigated for reducing loads in wind turbines [S9], [S10].

Information about the wind inflow is beneficial for controllers aimed at reducing loads. In [18], disturbance accommodating control is shown to mitigate blade loads assuming the wind inflow contains vortical coherent turbulent structures. Control to reduce overspeed and mitigate loads in response to extreme wind gusts is presented in [S11], where wind speed and direction at each blade are estimated.

Feedforward or model predictive control is another approach to improving disturbance rejection when the incoming wind profile deviates from the expected profile [11], [38], [S12]–[S19]. New wind measurement sensing technologies may improve feedforward control performance compared to feedforward controllers using estimates of the disturbance or wind deviation. For instance, there is interest in evaluating the potential of light

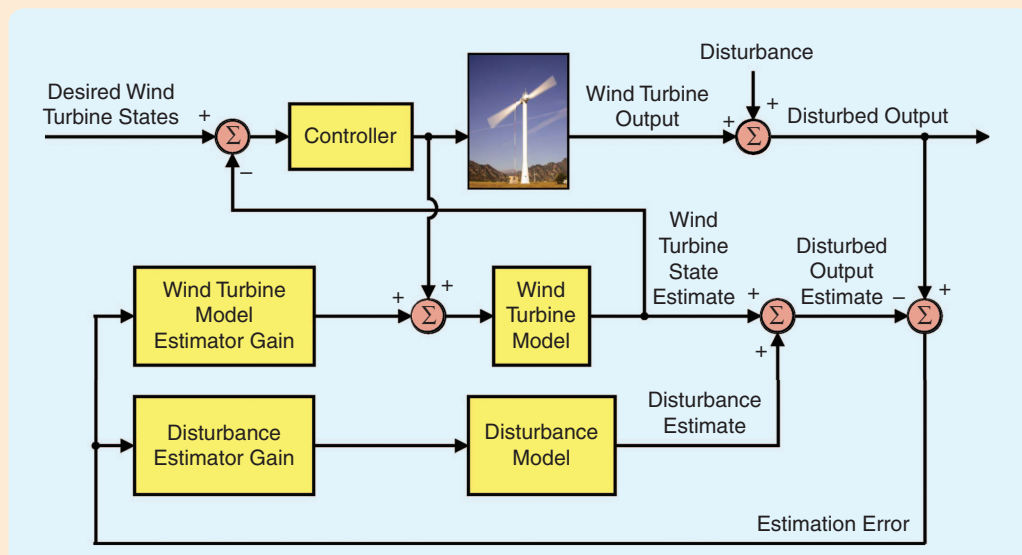


FIGURE S1 Disturbance accommodating control (DAC) applied to a wind turbine. Using a disturbance model, estimates of both the wind turbine state and disturbance are computed, and the wind turbine state estimate is used with a state-feedback controller to cause the wind turbine to track the desired turbine state reference inputs. DAC is applied to mitigate turbine loads and regulate rotor speed.

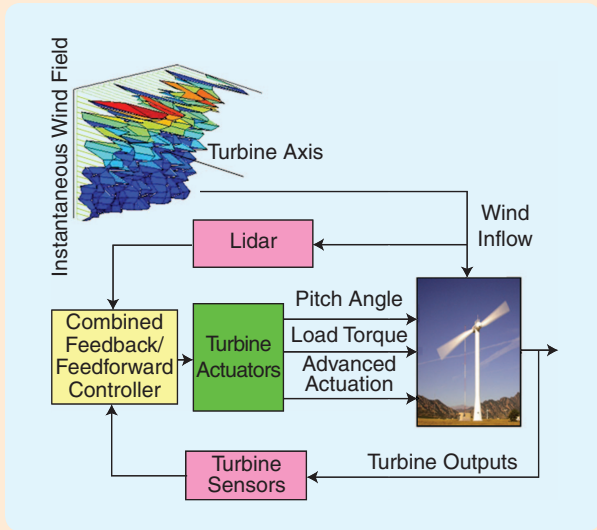


FIGURE S2 Wind turbine advanced control schematic. The wind inflow is measured by a lidar unit, providing a new measurement that can be used in control. Also shown is the possibility of new actuators compared to the baseline generator torque, blade pitch, and yaw. Multi-input, multi-output strategies can be used in this configuration.

Figure S2 can enable feedforward pitch control and feedforward torque control to improve performance. Advanced wind turbine controllers are further discussed and compared in [37].

As turbines become larger and blades longer, turbine manufacturers might build turbines that allow for different pitch angles at different radial positions along the blades relative to the standard blade twist angle. In this case, separate actuators and controllers might be necessary. Turbine manufacturers and researchers are also investigating actuators in addition to pitch motors to modify the aerodynamics of the turbine blade. For example, microtabs, trailing edge flaps, and synthetic jets or tiny valves to allow pressurized air to flow out of the blade can change the flow of the air across the blade, thus affecting the lift and drag coefficients and providing another possibility for control [S21]–[S23]. Advanced rotor concepts fall in two categories [S24], namely, devices to alter the local blade aerodynamic properties and geometry control by means of extendable blades. MIMO controllers for these advanced rotor concepts are based on linear state-space methods in conjunction with individual blade pitch control [S24]. Models for advanced rotor control design must go beyond those described in the section “Turbine Modeling”; see [S25].

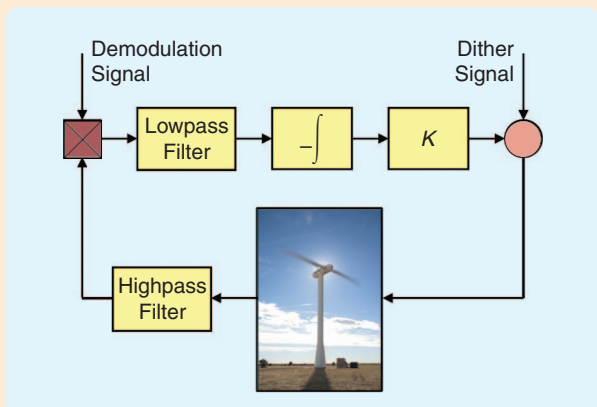


FIGURE S3 Extremum seeking control (ESC) for a wind turbine. Using rotor power as the turbine output and perturbing the blade pitch angle β and torque control gain K setpoints, ESC seeks to increase energy capture compared to a fixed-setpoint control [S35].

ENERGY CAPTURE

Maximum power point tracking (MPPT) [S26], [S27] is used to compensate for unknown or time-varying parameters, which are sometimes the cause of poor efficiency. Reference [S28] describes an MPPT controller whose goal is to maximize output power and generator efficiency without the need for a low-speed or high-speed shaft encoder, eliminating concern about sensor reliability.

Intelligent control strategies for energy optimization include the data-mining methods given in [S29], which also consider the power demand from the utility grid, as well as techniques such as the Wilcoxon radial basis function network with hill climbing [S30]. Reference [S31] compares the sliding mode observer with the model reference adaptive system (MRAS) and neural network strategies in terms of robustness against parameter variations. Neural network techniques can also be used to forecast the wind to achieve higher energy conversion efficiency [S32].

Extremum seeking control (ESC) [S33], [S34] provides a technique for online optimization. In [S35], a multivariable ESC strategy tested in simulation under field-recorded wind speed conditions is shown to increase energy capture compared to a baseline that does not include optimization. The two optimized variables are the torque control gain K (10) and the blade pitch angle β . ESC for a wind turbine is illustrated in Figure S3, where the turbine power is passed through a highpass filter, multiplied by a demodulation signal, and the resulting signal is passed through a lowpass filter. The lowpass filter output is integrated and multiplied by a gain, which could also be a transfer function. Finally, a dither signal perturbs the inputs to

detection and ranging sensors, known as lidars, for wind turbine control [11], [S13], [S16]. Lidar has been used in meteorology since the 1970s to measure wind speed profiles for monitoring hurricanes and wind conditions around airports. Lidar systems based on solid-state sources and off-the-shelf telecommunications equipment allow for inexpensive deployment, modularity, and improved reliability [14]–[17], [S20].

Depending on the particular type of technology used, lidar sensors can provide quantities representing the wind speed and direction and various wind turbulence and shear parameters. A measurement of the wind profile over the entire rotor plane in

the turbine, in this case β and K . The effect on turbine power of this perturbation can be overwhelmed by the changing wind speed input, and transient response can be improved by resetting the integrator or the highpass filter. Integrator antiwindup is also included to accommodate time periods during which the pitch or torque signals are saturated in Region 2 and Region 3, respectively.

Because the optimal rotor speed for energy capture is a function of the wind speed, various control techniques use a measurement of the wind speed input to maximize energy capture [S36]–[S37]. The advancement of lidar technologies might make these measurement-based controllers feasible.

According to [S38] energy-optimization techniques must consider the difference between the efficiency of conversion from wind to rotor (aerodynamic) and wind to generator (aerodynamic, mechanical, and electrical), since optimizing aerodynamic efficiency is not equivalent to optimizing system efficiency from the aerodynamics to the electrical system.

CONTROLLERS WITH MIXED OR ADDITIONAL GOALS

Controllers designed for both energy capture and load reduction include a LQG-based approach [S39] and a model reference adaptive controller to optimize energy capture and regulate rotor speed under parameter uncertainty [41].

Some concepts for modeling, design, and control of wind turbines are borrowed from the helicopter industry [S40]. Although rotating, pitchable blades are a common element, the dynamics and aerodynamics of the helicopter blades differ from those on the slower wind turbine such that controllers must be designed differently.

Another emerging area for wind turbine control is thermal control for anti-icing [S41]–[S43]. Since geographical regions where strong winds prevail are often in cold weather climates, the growth of wind farms in cold regions is faster than the global growth rate of installed wind capacity, and hence the need for thermal control techniques for anti-icing is increasing.

with the wind, provides active yaw control actuation for large turbines. However, due to dangerous gyroscopic forces, HAWTs must not be yawed at high rates. Consequently, the maximum yaw rate of a large turbine is typically limited to less than $1^\circ/\text{s}$. Thus, investigation of advanced controllers for yaw control provides less potential for benefit compared to advanced controllers for the remaining actuators.

The second type of actuator is the generator (see Figure 10), which, depending on the generator and power processing equipment, can be commanded to follow a desired torque or load. Generator torque control, performed using the power electronics, determines how much torque is extracted from the turbine. The generator and power electronics produce a load torque based on the separation of magnets in the generator's stator and rotor, which should

REFERENCES

- [S1] E. A. Bossanyi, "Wind turbine control for load reduction," *Wind Energy*, vol. 6, pp. 229–244, 2003.
- [S2] E. A. Bossanyi, "Further load reductions with individual pitch control," *Wind Energy*, vol. 8, pp. 481–485, 2005.
- [S3] M. Balas, Y. J. Lee, and L. Kendall, "Disturbance tracking control theory with application to horizontal axis wind turbines," in *Proc. AIAA/ASME Wind Energy Symp.*, Reno, NV, 1998, pp. 95–99.
- [S4] H. Namik and K. Stol, "Disturbance accommodating control of floating offshore wind turbines," in *Proc. AIAA/ASME Wind Energy Symp.*, Orlando, FL, 2009, AIAA 2009-483.
- [S5] G. A. Parker and C. D. Johnson, "Improved speed regulation and mitigation of drive-train torsion fatigue in flexible wind turbines, using disturbance utilization control: Part one," in *Proc. 41st Southeastern Symp. System Theory*, Tullahoma, TN, 2009, pp. 171–176.
- [S6] C. D. Johnson, "Theory of disturbance-accommodating controllers," in *Control and Dynamic Systems*, C. T. Leondes, Ed. New York: McGraw-Hill, 1976, vol. XII.
- [S7] K. Z. Ostergaard, J. Stoustrup, and P. Brath, "Linear parameter varying control of wind turbines covering both partial load and full load conditions," *Int. J. Robust Nonlinear Control*, vol. 19, pp. 92–116, 2009.
- [S8] A. Kumar and K. Stol, "Simulating feedback linearization control of wind turbines using high-order models," *Wind Energy*, vol. 13, no. 5, pp. 419–432, 2010.
- [S9] M. A. Rotea, M. A. Lackner, and R. Saheba, "Active structural control of offshore wind turbines," in *Proc. AIAA/ASME Wind Energy Symp.*, Orlando, FL, 2010, AIAA 2010-1000.
- [S10] M. A. Lackner and M. A. Rotea. (2011). Passive structural control of offshore wind turbines. *Wind Energy*, vol. 14 [Online]. Available: <http://onlinelibrary.wiley.com/doi/10.1002/we.426/full>
- [S11] S. Kanev and T. van Engelen, "Wind turbine extreme gust control," *Wind Energy*, vol. 13, pp. 18–35, 2010.
- [S12] A. A. Kumar and K. A. Stol, "Scheduled model predictive control of a wind turbine," in *Proc. AIAA/ASME Wind Energy Symp.*, Orlando, FL, 2009, AIAA 2009-481.
- [S13] M. M. Hand, A. D. Wright, L. J. Fingersh, and M. Harris, "Advanced wind turbine controllers attenuate loads when upwind velocity measurements are inputs," in *Proc. AIAA/ASME Wind Energy Symp.*, Reno, NV, 2006, AIAA 2006-603.
- [S14] J. H. Laks, L. Y. Pao, and A. Wright, "Combined feedforward/feedback control of wind turbines to reduce blade flap bending moments," in *Proc. AIAA/ASME Wind Energy Symp.*, Orlando, FL, 2009, AIAA 2009-687.
- [S15] K. Selvam, S. Kanev, J. W. van Wingerden, T. van Engelen, and M. Verhaegen, "Feedback-feedforward individual pitch control for wind turbine load reduction," *Int. J. Robust Nonlinear Control*, vol. 19, no. 1, pp. 72–91, 2009.
- [S16] D. Schlipf and M. Kuhn, "Prospects of a collective pitch control by means of predictive disturbance compensation assisted by wind speed

not be confused with the turbine's rotor. The type of magnets and methods for producing the separation depend on the type of generator and power electronics. Although the net torque on the rotor depends on the input torque from the wind and the load torque from the generator, the generator torque can be used to affect the acceleration and deceleration of the rotor. The fast time constant of the generator torque, which is at least an order of magnitude faster than that of the rotor speed, makes generator torque an effective actuator for controlling rotor speed.

The third type of actuator is the blade-pitch motor. Figure 11 shows the three pitch motors of the three-bladed controls advanced research turbine (CART3) at NREL. Like CART3, the majority of utility-scale wind turbines have three blades and thus three pitch motors. Figure 12 shows

- measurements," in *Proc. DEWEK (German Wind Energy Conf.)*, 2008, pp. 1–4.
- [S17] F. Dunne, L. Y. Pao, A. Wright, B. Jonkman, and N. Kelley, "Combining standard feedback controllers with feedforward blade pitch control for load mitigation in wind turbines," in *Proc. AIAA/ASME Wind Energy Symp.*, Orlando, FL, 2010, AIAA 2010-250.
- [S18] J. H. Laks, L. Y. Pao, E. Simley, A. Wright, N. Kelley, and B. Jonkman, "Model predictive control using preview measurements from lidar," in *Proc. AIAA/ASME Wind Energy Symp.*, Orlando, FL, Jan. 2011, AIAA-2011-813, pp. 1–20.
- [S19] E. Simley, L. Y. Pao, R. Frehlich, B. Jonkman, and N. Kelley, "Analysis of wind speed measurements using coherent lidar for wind preview control," in *Proc. AIAA/ASME Wind Energy Symp.*, Orlando, FL, Jan. 2011, AIAA-2011-263, pp. 1–16.
- [S20] M. R. Huffaker and R. M. Hardesty, "Remote sensing of atmospheric wind velocities using solid-state and CO₂ coherent laser systems," *Proc. IEEE*, vol. 84, no. 2, pp. 181–204, 1996.
- [S21] M. A. Lackner and G. A. M. van Kuik, "A comparison of smart rotor control approaches using trailing edge flaps and individual pitch control," *Wind Energy (Special Issue: Smart Blades)*, vol. 13, no. 2-3, pp. 117–134, 2010.
- [S22] S. Johnson, J. Baker, C. van Dam, and D. Berg, "An overview of active load control techniques for wind turbines with an emphasis on microtabs," *Wind Energy*, vol. 13, pp. 239–253, 2010.
- [S23] V. Maldonado, J. Farnsworth, W. Gressick, and M. Amitay, "Active control of flow separation and structural vibrations of wind turbine blades," *Wind Energy (Special Issue: Smart Blades)*, vol. 13, no. 2-3, pp. 221–237, 2010.
- [S24] T. J. McCoy and D. A. Griffin, "Control of rotor geometry and aerodynamics: Retractable blades and advanced concepts," *Wind Eng.*, vol. 32, no. 1, pp. 13–26, 2008.
- [S25] J. Rice and M. Verhaegen, "Robust and distributed control of a smart blade," *Wind Energy*, vol. 13, pp. 103–116, 2010.
- [S26] S. Bhowmik, R. Spee, and J. Enslin, "Performance optimization for doubly-fed wind power generation systems," *IEEE Trans. Ind. Appl.*, vol. 35, no. 4, pp. 949–958, 1999.
- [S27] A. M. Howlander, N. Urasaki, K. Uchida, A. Yona, T. Senju, C.-H. Kim, and A. Y. Saber, "Parameter identification of wind turbine for maximum power-point tracking control," *Electric Power Compon. Syst.*, vol. 38, pp. 603–614, 2010.
- [S28] T. Senju, Y. Ochi, Y. Kikunaga, M. Tokudome, A. Yona, E. B. Muhando, N. Urasaki, and T. Funabashi, "Sensor-less maximum power point tracking control for wind generation system with squirrel-cage induction generator," *Renewable Energy*, vol. 34, pp. 994–999, 2009.
- [S29] A. Kusiak, W. Li, and Z. Song, "Dynamic control of wind turbines," *Renewable Energy*, vol. 35, pp. 456–463, 2010.
- [S30] W.-M. Lin and C.-M. Hong, "Intelligent approach to maximum power point tracking control strategy for variable-speed wind turbine generation system," *Energy*, vol. 35, pp. 2440–2447, 2010.
- [S31] J. Brahmi, L. Krichen, and A. Ouali, "A comparative study between three sensorless control strategies for PMSG in wind energy conversion system," *Appl. Energy*, vol. 86, pp. 1565–1573, 2009.
- [S32] M. Narayana, G. Putrus, M. Jovanovic, and M. P. S. Leung, "Predictive control of wind turbines by considering wind speed forecasting techniques," in *Proc. 44th International Universities Power Engineering Conf.*, UPEC2009, Glasgow, Scotland, 2009, pp. 1–4.
- [S33] M. Krstic, "Performance improvement and limitations in extremum seeking control," *Syst. Control Lett.*, vol. 39, no. 5, pp. 313–326, 2000.
- [S34] M. Krstic and H. H. Wang, "Stability of extremum seeking feedback for general nonlinear dynamic systems," *Automatica*, vol. 36, no. 4, pp. 595–601, 2000.
- [S35] J. Creaby, Y. Li, and J. E. Seem, "Maximizing wind turbine energy capture using multivariable extremum seeking control," *Wind Eng.*, vol. 33, no. 4, pp. 361–388, 2009.
- [S36] N. A. Cutululis, E. Ceanga, A. D. Hansen, and P. Sorensen, "Robust multi-model control of an autonomous wind power system," *Wind Energy*, vol. 9, pp. 399–419, 2006.
- [S37] H. Geng and G. Yang, "Output power control for variable-speed variable-pitch wind generation systems," *IEEE Trans. Energy Conversion*, vol. 25, no. 2, pp. 494–503, June 2010.
- [S38] C. Vlad, I. Munteanu, A. I. Bratcu, and E. Ceanga, "Output power maximization of low-power wind energy conversion systems revisited: Possible control solutions," *Energy Convers. Manage.*, vol. 51, pp. 305–310, 2010.
- [S39] E. Muhando, T. Senju, E. Omine, T. Funabashi, and C. Kim, "Modelling-based approach for digital control design for nonlinear WECS in the power system," *Wind Energy*, vol. 13, no. 6, pp. 543–557, 2010.
- [S40] F. Stoddard, "Wind turbine blade technology: A decade of lessons learned," in *Proc. World Renewable Energy Congr.*, Reading, England, 1990, pp. 1570–1578.
- [S41] X. Wang. (2008). Convective heat transfer and experimental icing aerodynamics of wind turbine blades, Ph.D. dissertation, Univ. Manitoba [Online]. Available: <http://mspace.lib.umanitoba.ca/handle/1993/3082>
- [S42] T. Laakso, I. Baring-Gould, M. Durstewitz, R. Horbaty, A. Lacroix, E. Peltola, G. Ronsten, L. Tallhaug, and T. Wallenius. (2009). State-of-the-art of wind energy in cold climates. Int. Energy Agency Report [Online]. Available: <http://arcticwind.vtt.fi/>
- [S43] S. Barber, Y. Wang, S. Jafari, N. Chokani, and R. S. Abhari, "The effect of icing on wind turbine performance and aerodynamics," in *Proc. European Wind Energy Conf.*, Warsaw, Poland, 2010, pp. 1–11.

operational blade pitch angle data from CART2, a two-bladed, 600-kW wind turbine with a 43-m diameter rotor at NREL's NWTC. Data collection was performed during a normal shut-down event when the wind speed decreased into Region 1. In this case, the pitch rate is restricted to approximately 5°/s. The lag between the commanded and actual pitch angle can be represented by a first-order filter.

Wind turbine blades can be controlled to pitch collectively or independently. Varying the blade pitch angle changes the aerodynamic torque due to the wind, and pitch motors are fast enough to be used to control rotor speed and power and mitigate loads on blades and towers. The 600-kW CART2 and CART3 have maximum pitch rates of 18°/s, but maximum pitch rates are slower for larger turbines and are closer to 8°/s for 5-MW turbines.

Variable-pitch turbines can limit power by pitching either to stall or to feather, whereas fixed-pitch turbines typically limit power by entering the aerodynamic stall regime above rated wind speed. A blade in full feather is one in which the leading edge of the blade points directly into the wind. The benefits of pitching to feather versus pitching to stall are discussed in [5] and [22].

Turbine Modeling

When only the rotor speed is of interest, a first-order model of the wind turbine is given by

$$\dot{\omega} = \frac{1}{J}(\tau_{\text{aero}} - \tau_{\text{load}}), \quad (4)$$

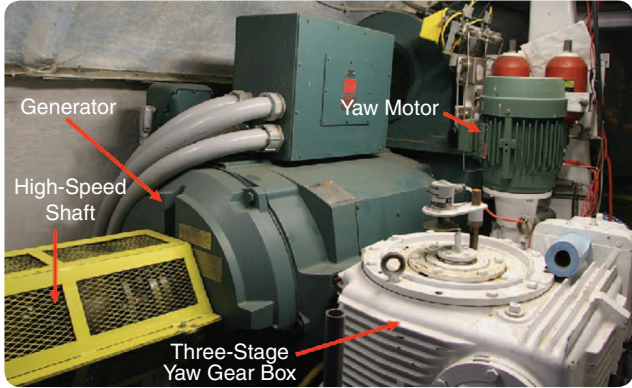


FIGURE 10 Inside the CART3 nacelle. The high-speed shaft is inside the yellow cage at left, the generator is the large green unit in the middle, the yaw motor is the smaller green unit toward the right, and the three-stage yaw gearbox is the large white box in the lower right. A larger gearbox (not shown) connects the high-speed shaft on the left to the low-speed shaft and rotor. (Photo courtesy of Lee Jay Fingersh of NREL.)

where ω is the rotor velocity, J is the rotational inertia of the turbine, τ_{aero} is the aerodynamic torque, and τ_{load} is the electrical load.

The tip-speed ratio is the ratio of the tangential speed of the blade tip to the wind speed

$$\lambda = \frac{\omega R}{v}, \quad (5)$$

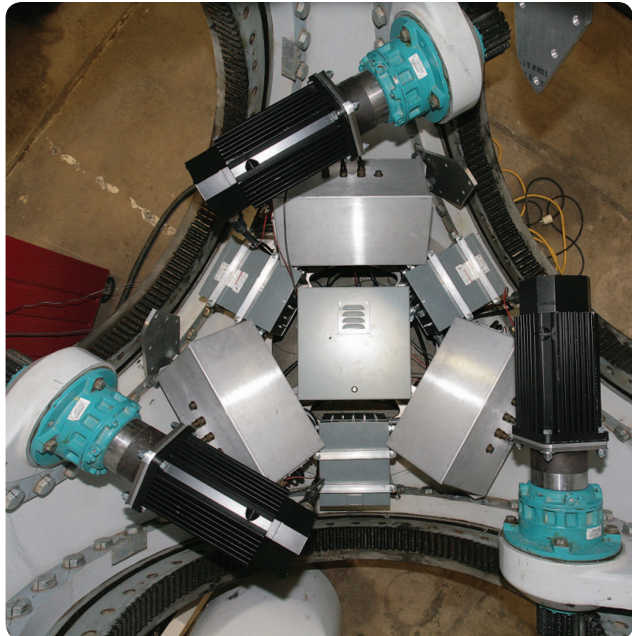


FIGURE 11 Pitch motors mounted inside CART3's hub. This photo, taken prior to installation on the nacelle, is looking upwind from the turbine. The control circuitry boxes and gears are also visible. Like many utility-scale turbines, CART3 is equipped with independent blade pitch capability. (Photo courtesy of Lee Jay Fingersh of NREL.)

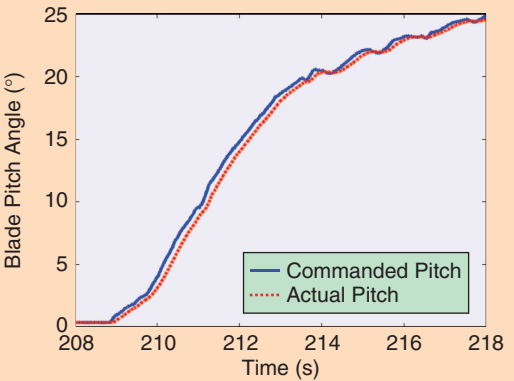


FIGURE 12 Operating data from CART2, the two-bladed Controls Advanced Research Turbine at NREL's NWTC. The commanded pitch and actual pitch angles are shown during a normal shutdown event as the blades are pitched from -1° to 90° , although only the first 10 s of the shutdown event are plotted. The lag between the two signals can be represented by a first-order filter.

where R is the rotor radius, the instantaneous wind speed v is time varying, and the rotor angular velocity ω , most commonly known as the rotor speed, is time varying for a variable-speed turbine.

The power coefficient C_p , which is given by (1) and is a function of the turbine's blade pitch angle β and tip-speed ratio λ , is needed to determine τ_{aero} in (4). The relationship between the power coefficient C_p and the tip-speed ratio λ is a turbine-specific nonlinear function but usually has a downward parabolic shape. The surface characterizing C_p for the CART3 is shown in Figure 13.

The aerodynamic torque τ_{aero} is given by

$$\tau_{\text{aero}} = \frac{1}{2} \rho A R \frac{C_p(\lambda, \beta)}{\lambda} v^2. \quad (6)$$

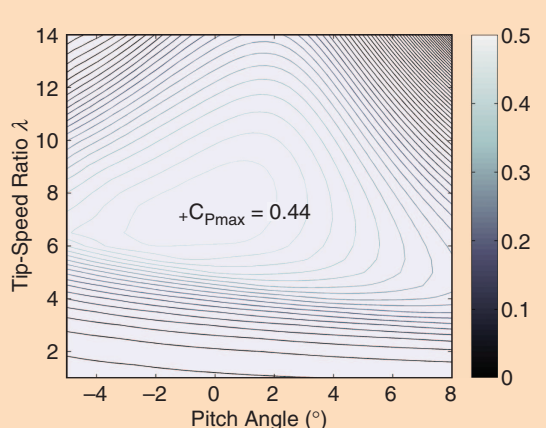


FIGURE 13 C_p for CART3. The maximum power coefficient $C_{p_{\text{max}}} = 0.4438$ for CART3 occurs at the tip-speed ratio $\lambda_* = 7.0$ and the blade pitch angle $\beta_* = -0.75^\circ$. The Region 2 control objective is to operate as close to $C_{p_{\text{max}}}$ as possible to maximize aerodynamic efficiency.

Linearizing τ_{aero} around the operating point (ω_{op} , β_{op} , v_{op}) yields

$$\tau_{\text{aero}} \approx \tau_{\text{aero}_{\text{op}}} + \Gamma_{\omega}\delta\omega + \Gamma_{\beta}\delta\beta + \Gamma_v\delta v, \quad (7)$$

where $\Gamma_{\omega} = \frac{\partial\tau_{\text{aero}}}{\partial\omega} \Big|_{\omega=\omega_{\text{op}}}$, $\Gamma_{\beta} = \frac{\partial\tau_{\text{aero}}}{\partial\beta} \Big|_{\beta=\beta_{\text{op}}}$, and $\Gamma_v = \frac{\partial\tau_{\text{aero}}}{\partial v} \Big|_{v=v_{\text{op}}}$.

The linearized rotor-speed-perturbation equation is then given by

$$\delta\dot{\omega} \approx \frac{\Gamma_{\omega}}{J}\delta\omega + \frac{\Gamma_{\beta}}{J}\delta\beta + \frac{\Gamma_v}{J}\delta v. \quad (8)$$

A pitch controller can be designed based on the pitch-angle perturbation $\delta\beta$ to regulate rotor speed, where the perturbed wind speed δv is the disturbance.

Unfortunately, neither the reduction to a single degree of freedom nor the linearization to a single operating point is reasonable for large, flexible structures operating under diverse conditions, and thus controllers designed solely using (8) are unlikely to work. Some of the engineering design tools used by wind turbine manufacturers, developers, and control engineers include [23]–[31]. Figure 14 [29] shows various turbine modeling areas and the flow of information in the wind turbine modeling codes FAST [24] and ADAMS [31]. Turbulent inflow, aerodynamics, hydrodynamics (for offshore turbines only), and foundation dynamics must all be considered to determine how the structural dynamics and control systems perform.

Control Loops

The primary Region 2 control objective for a variable-speed wind turbine is to maximize the power coefficient C_p . As shown in Figure 13, the turbine operates at its highest aerodynamic efficiency point $C_{p_{\max}}$ at a specific pitch angle and tip-speed ratio. Using electromechanical or hydraulic actuators, pitch angle can be maintained at the optimally efficient pitch angle. However, tip-speed ratio depends on the incoming wind speed v and is therefore continually changing. Thus, Region 2 control is primarily concerned with varying the rotor speed to track the wind speed.

On utility-scale wind turbines, Region 3 control is typically performed by means of a pitch control loop such as the one shown in Figure 6. In Region 3, the primary objective is to limit the turbine power and rotor speed so that safe electrical and mechanical loads are not exceeded. Pitching the blades or yawing the turbine out of the wind can reduce the aerodynamic torque below what would otherwise be available from an increase in wind speed, thereby limiting the power P , which is related to rotor speed ω and aerodynamic torque τ_{aero} by

$$P = \tau_{\text{aero}}\omega. \quad (9)$$

To hold the power and rotor speed constant, the aerodynamic torque must also be controlled to a constant value even as wind speed varies. In Region 3, the pitch control loop regulates the rotor speed ω to the turbine's rated speed so that the turbine operates at its rated power.

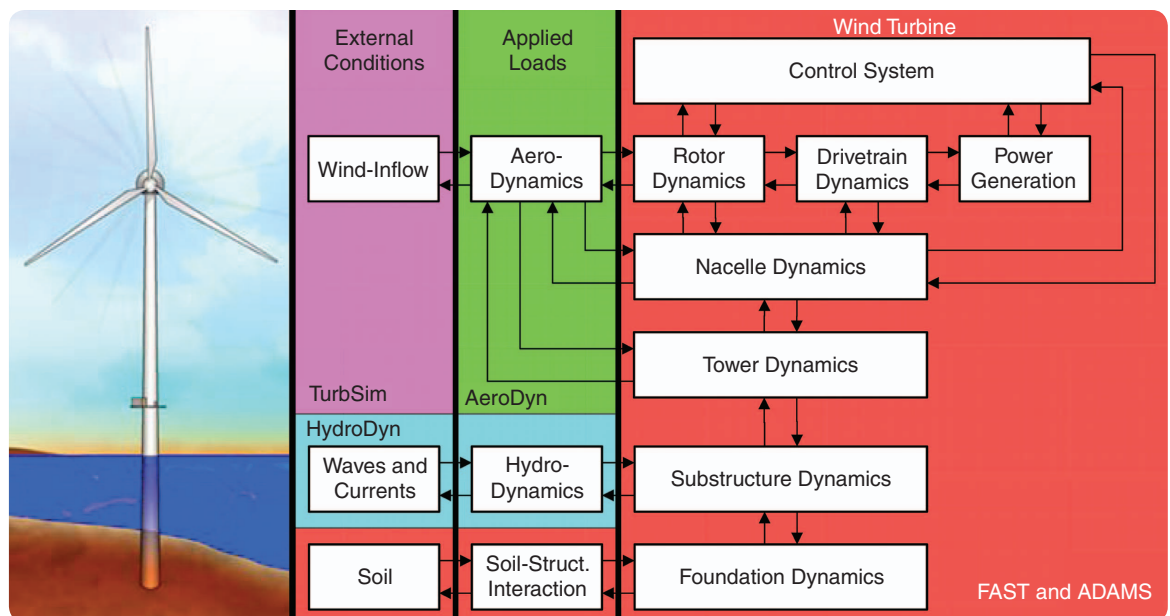


FIGURE 14 Modeling hierarchy for the NREL design codes for wind turbine control design [27], [29]. External conditions such as the wind input are generated in TurbSim, which interacts with AeroDyn for aerodynamic computations. AeroDyn connects with FAST and ADAMS at the rotor, nacelle, and tower levels. Substructure and foundation dynamics can also be modeled using this suite of software. (Reproduced with permission from [29].)

Modeling and Control of Wind Farms

Wind turbines are often located with other turbines in wind farms to reduce costs by taking advantage of economies of scale. Figure S4 shows turbines in a linear array. Turbines on wind farms can be located along a single line, in multiple lines, in clusters, in grids, or in configurations based on geographical features, prevailing wind direction, access requirements, environmental effects, safety, prior and future land use including farmland and ranchland, and visual impact.

From a control systems perspective, wind farm research is focused mainly on either control of the electricity generated by the turbines [5] or coordinated control of the energy captured by individual turbines to minimize the negative effect of aerodynamic interaction [S44]–[S46]. Although various types of generators can be used [6], doubly-fed induction generators are increasingly used in wind turbines [S28], [S47]–[S49]. Standards governing the wind farm's interconnection to the utility grid vary by location [S50], but typically it is expected that wind farms are equipped with strategies for voltage control, do not contribute to grid faults, and are not damaged by grid faults. Voltage stability and the uninterrupted operation of a wind farm connected to an electric grid during a grid fault is an active area of research [S49], as is the use of wind turbines to protect against grid faults [S51]–[S53]. Individual turbines and older farms with comparatively small capacity had little effect on the grid.

Control of active and reactive power supplied by wind farms to the utility grid is also a major area of research [S47], [S54]. Experiences at Denmark's Horns Rev [S55], the first wind farm equipped with advanced control of both active and reactive power, can provide guidelines for newer wind farms. Lyapunov-based strategies can be used to damp the network electromechanical oscillations of a wind farm's power output while trying to minimize the number of sensors required in the farm [S56]. Electrical system control over multiple levels is typically used to achieve multiple objectives on a wind farm [S48], [S57] and relies on models of wind farms from an electrical perspective [S58], [S59].

The aerodynamic interaction of turbines on a wind farm is not as well understood as the electrical interconnection of the turbines. While wind farms help reduce the average cost of energy compared to widely dispersed turbines due to econo-



FIGURE S4 Wind farm in Galicia, Spain. Aerodynamic and electrical interaction among turbines on a wind farm can result in energy-capture losses. Better modeling and coordinated control of arrays of multiple turbines can recover some of these losses. (Used with permission from [S62].)

mies of scale, aerodynamic interaction among turbines can decrease the total energy converted to electricity compared to the same number of isolated turbines operating under the same wind inflow conditions [29]. Turbines on a wind farm are typically spaced farther apart in the direction parallel to the prevailing wind direction, known as downwind spacing, than in the perpendicular direction, known as crosswind spacing, as shown in Figure S5. Downwind spacing is often eight to ten rotor diameters, and crosswind spacing is often four to five rotor diameters, although the exact distances chosen vary with geography and additional factors. Shorter crosswind spacing distances can reduce land costs and are beneficial at locations where the frequency distribution of the wind direction is skewed heavily toward the prevailing direction.

The array efficiency η_A of a wind farm is given by

$$\eta_A = \frac{E_A}{E_T N},$$

where E_A is the annual energy of the array, E_T is the annual energy of one isolated turbine, and N is the number of turbines in the wind farm. An array efficiency greater than 90% can be achieved when downwind spacings of eight to ten rotor diameters and crosswind spacings of five rotor diameters are used [5].

Since wind turbines can slow the wind over a distance of 5–20 km [S60], turbines arranged in a wind farm interact aerodynamically. Coordinated control of the turbines can reduce

FEEDBACK CONTROL

We now describe control algorithms for the torque control and pitch control blocks of Figure 6. As depicted in Figure 6, both control loops typically use only rotor speed feedback. In the standard configuration, the remaining sensors and measurements discussed in the section "Sensors" are used only for supervisory control and fault detection purposes. For a more detailed description of wind turbine control, including the four combinations of variable and fixed pitch together with variable and fixed speed, see [22].

Generator Torque Control

Various proprietary generator torque controllers are used by the wind industry. A standard torque controller used on CART2 and CART3 sets the generator torque τ_c , which is also the load torque τ_{load} in (4), as

$$\tau_c = K\omega^2, \quad (10)$$

where K is given by

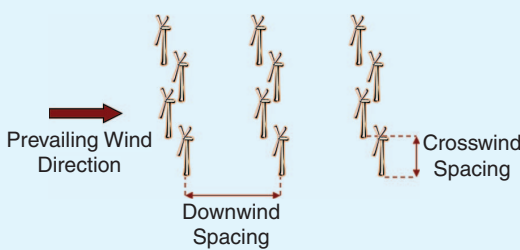


FIGURE S5 Downwind and crosswind spacing of wind turbines in a farm. Turbines are normally arranged with larger distances between turbines in the prevailing wind direction than in the perpendicular direction. Although the shorter crosswind spacing reduces land use, energy capture can be compromised when the wind comes from a direction other than the prevailing one.

the negative effects caused by this aerodynamic interaction. It can be shown [S61] that having each wind turbine in an array extract as much energy as possible does not lead to maximal total overall energy capture across the entire array because the turbines on the upwind side of the farm extract too much energy, slowing the wind too much before it reaches the remaining turbines. The spatial variation of turbines on a wind farm often results in power smoothing, where the standard deviation of the power produced by multiple turbines is less than the standard deviation of the power produced by each individual turbine [5]. This effect is caused by different wind gusts and lulls hitting different turbines on the farm at different times.

REFERENCES

- [S44] M. Liu, M. Yooke, and T. Myers, "Mathematical model for the analysis of wind-turbine wakes," *J. Energy*, vol. 7, pp. 73–78, 1983.
- [S45] M. Steinbuch, W. W. de Boer, O. H. Bosgra, S. A. W. M. Peters, and J. Ploeg, "Optimal control of wind power plants," *J. Wind Eng. Ind. Aerodyn.*, vol. 27, pp. 237–246, 1988.
- [S46] S. Frandsen, "On the wind speed reduction in the center of large clusters of wind turbines," *J. Wind Eng. Ind. Aerodyn.*, vol. 39, pp. 251–265, 1992.
- [S47] L. M. Fernandez, C. A. Garcia, and F. Jurado, "Comparative study on the performance of control systems for doubly fed induction generator (DFIG) wind turbines operating with power regulation," *Energy*, vol. 33, pp. 1438–1452, 2008.
- [S48] A. D. Hansen, P. Srensen, F. Iov, and F. Blaabjerg, "Centralised power control of wind farm with doubly fed induction generators," *Renewable Energy*, vol. 31, pp. 935–951, 2006.
- [S49] W. Qiao, G. K. Venayagamoorthy, and R. G. Harley, "Real-time implementation of a statcom on a wind farm equipped with doubly fed induction generators," *IEEE Trans. Ind. Applicat.*, vol. 45, no. 1, pp. 98–107, 2009.
- [S50] C. Jauch, J. Matevosyan, T. Ackermann, and S. Bolik, "International comparison of requirements for connection of wind turbines to power systems," *Wind Energy*, vol. 8, no. 3, pp. 295–306, 2005.
- [S51] I. Erlich and M. Wilch, "Primary frequency control by wind turbines," in *Proc. Power and Energy Society General Meeting*, Minneapolis, MN, 2010, pp. 1–8.
- [S52] G. C. Tarnowski, P. C. Kjaer, S. Dalgaard, and A. Nyborg, "Regulation and frequency response service capability of modern wind power plants," in *Proc. Power and Energy Society General Meeting*, Minneapolis, MN, 2010, pp. 1–8.
- [S53] N. W. Miller and K. Clark, "Advanced controls enable wind plants to provide ancillary services," in *Proc. Power and Energy Society General Meeting*, Minneapolis, MN, 2010, pp. 1–8.
- [S54] C. F. Moyano and J. A. Pecas Lopes, "An optimization approach for wind turbine commitment and dispatch in a wind park," *Electric Power Syst. Res.*, vol. 79, pp. 71–79, 2009.
- [S55] J. Kristoffersen, "The Horns Rev wind farm and the operational experience with the wind farm main controller," *Revue E*, vol. 122, pp. 26–31, 2006.
- [S56] R. D. Fernandez, P. E. Battaiotto, and R. J. Mantz, "Wind farm non-linear control for damping electromechanical oscillations of power systems," *Renewable Energy*, vol. 33, pp. 2258–2265, 2008.
- [S57] J. L. Rodriguez-Amenedo, S. Arnaltes, and M. A. Rodriguez, "Operation and coordinated control of fixed and variable speed wind farms," *Renewable Energy*, vol. 33, pp. 406–414, 2008.
- [S58] E. Muljadi and C. P. Butterfield. (2004). Wind farm power system model development. *Proc. World Renewable Energy Conf.*, Denver, CO, pp. 1–8 [Online]. Available: <http://www.nrel.gov/docs/fy04osti/36199.pdf>
- [S59] E. Muljadi and B. Parsons. (2006). Comparing single and multiple turbine representations in a wind farm simulation. *Proc. European Wind Energy Conf.*, Athens, Greece, pp. 1–13 [Online]. Available: <http://www.nrel.gov/docs/fy06osti/39510.pdf>
- [S60] M. B. Christiansen and C. B. Hasager, "Wake effects of large offshore wind farms identified from satellite SAR," *Remote Sens. Environ.*, vol. 98, pp. 251–268, 2005. [S61] K. E. Johnson and N. Thomas, "Wind farm control: Addressing the aerodynamic interaction among wind turbines," in *Proc. American Control Conf.*, St. Louis, MO, 2009, pp. 2104–2109.
- [S62] arnejohs. Windpark in Galicia (2011). [Online]. Available: http://upload.wikimedia.org/wikipedia/commons/0/0c/Windpark_Galicia.jpg

$$K = \frac{1}{2} \rho \pi R^5 \frac{C_{p_{\max}}}{\lambda_*^3}, \quad (11)$$

and λ_* is the tip-speed ratio at the maximum power coefficient $C_{p_{\max}}$.

The torque control given by (10) and (11) can be shown to achieve $C_{p_{\max}}$. To analyze the closed-loop system, we combine (1)–(11) to obtain

$$\dot{\omega} = \frac{1}{2} \rho \pi R^5 \omega^2 \left(\frac{C_p}{\lambda^3} - \frac{C_{p_{\max}}}{\lambda_*^3} \right). \quad (12)$$

It follows from (12) that, if $C_p < (C_{p_{\max}}/\lambda_*^3)\lambda^3$, then $\dot{\omega} < 0$. On the other hand, if $C_p > (C_{p_{\max}}/\lambda_*^3)\lambda^3$, then $\dot{\omega} > 0$. Thus, the control law given by (10) and (11) causes the turbine to accelerate toward the desired setpoint λ_* when the rotor speed is too slow and decelerate when the rotor speed is too fast. The representation of (12) is shown graphically in Figure 15. For further details, see [32].

Figure 16 shows CART2 operational data of the measured high-speed shaft generator speed, the control torque signal given by (10), and the pitch control signal. For the first 50 s,

Offshore Wind Turbines

A vast offshore wind resource exists worldwide [S63], [S64]. In the United States the offshore resource is estimated to be approximately 900 GW of installed capacity [S64]. Several advantages exist for installing wind turbines offshore compared to onshore. First, wind tends to blow more strongly and consistently offshore, with less turbulence and smaller shear at sea than on land. Second, the sizes of offshore wind turbines are not limited by the logistical constraints of road or rail transportation. Third, the visual and noise disturbances of wind turbines can be avoided if the turbines are installed a sufficient distance from shore. Furthermore, vast expanses of uninterrupted open sea are available, saving land for other uses.

Fixed-bottom offshore turbines present special control challenges compared to land-based turbines since the flexible tower is excited by ocean waves. To ensure that waves do not excite dominant tower bending modes, either the initial turbine design must account for the wave excitation or advanced control techniques must be used.

For many countries such as the United States, the majority of the offshore wind resource potential is in deep water greater than about 30-m deep [S65]. Commercially-available monopiles driven into the seabed and concrete gravity bases used in fixed-bottom shallow water, which is less than approximately 20 m, are not economically feasible for these newer deep water installations. As shown in Figure S6, at some depth floating support platforms are more cost effective than fixed-bottom installations. Numerous floating platform configurations, such as those shown in Figure S7, are possible, including various configurations already used in the

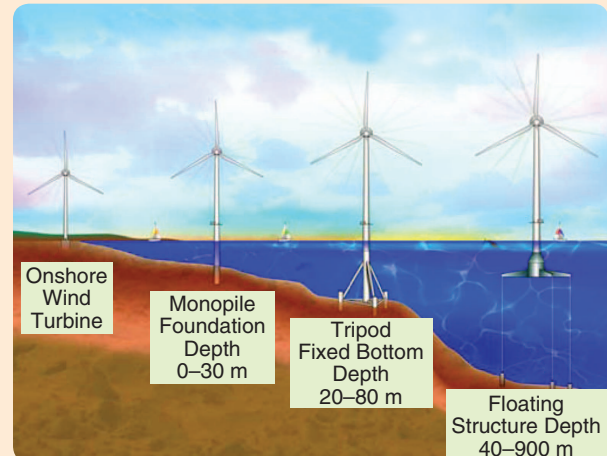


FIGURE S6 Wind turbine substructure designs for use onshore, in shallow water, and in deepwater. As water depth increases, substructure costs also increase, and taller substructure plus tower systems experience more significant wave load disturbances compared to shallow-bottom turbines. (Image courtesy of NREL.)

offshore oil and gas industries. Research includes evaluating various floating support platform configurations, deriving models of the coupled aeroelastic and hydrodynamics responses of offshore wind turbines, and developing comprehensive simulation tools [S65]–[S68].

New research is required to determine whether any of these floating offshore platform concepts are technically or economically feasible for offshore wind turbines. Fundamental issues of controllability and observability of offshore wind turbines need

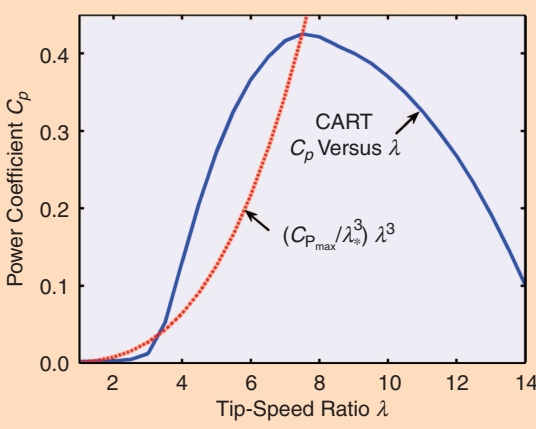


FIGURE 15 A plot of C_p versus λ for CART3. The blade pitch angle is fixed at $\beta = -0.75^\circ$. The turbine accelerates toward the optimal tip-speed ratio λ_* when the red dashed curve representing (12) is less than the blue solid curve and decelerates when the opposite is true.

the wind speed is low enough that control is based on (10). After that time, wind speeds are high enough that the rated speed of 1800 rev/min is reached, at which time the torque control signal is saturated and pitch control takes over to limit turbine power. The two steepest sections of the torque control signal at approximately 417 s and 427 s are due to the tower-resonance-avoidance controller described further in [21].

Pitch Control

In some commercial wind turbines, pitch control in Region 3 is performed using the proportional-integral-derivative (PID) collective pitch control law

$$\beta_e(t) = K_p \omega_e(t) + K_I \int_0^t \omega_e(\tau) d\tau + K_D \frac{d\omega_e(t)}{dt}, \quad (13)$$

where $\omega_e = \omega_d - \omega$ is the rotor speed error and the desired rotor speed is ω_d . Because of its sensitivity to measurement noise, the derivative term can be combined with a lowpass filter or set to $K_D = 0$, leaving just a PI pitch controller. The

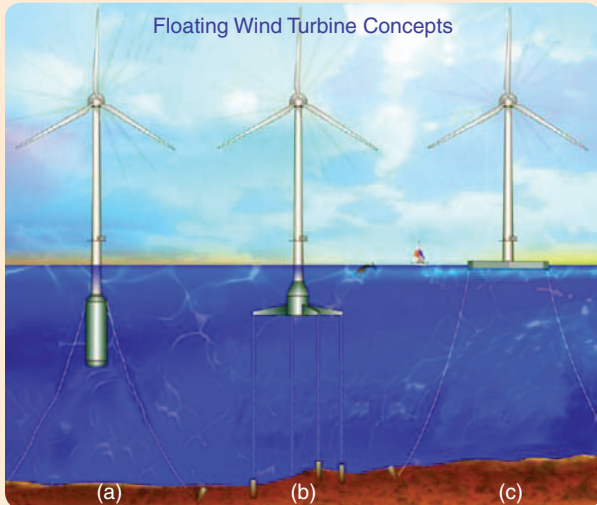


FIGURE S7 Floating platform configurations for deepwater offshore wind turbines. (a) Ballast stabilized spar-buoy with catenary mooring drag embedded anchors, (b) mooring line stabilized tension leg platform with suction pile anchors, and (c) buoyancy stabilized barge with catenary mooring lines. Due to the nature of the continental shelf around many countries, it is expected that the majority of future offshore wind turbines will be required to be floating. The additional degrees of freedom provided by floating configurations compared to fixed-bottom configurations lead to new control challenges. (Image courtesy of NREL.)

to be investigated. For example, we must determine whether deepwater offshore wind turbines are stabilizable or controllable using pitch control, generator torque control, and yaw control actuators that already exist in land-based wind turbines. If not, we must understand what additional actuators are needed to

enable stabilizability and controllability and what sensors are required to observe the parameters that enable effective feedback control performance. These fundamental questions must be answered before deepwater offshore wind turbines can be designed and deployed on large scales. Initial studies explore the extent to which individual blade pitch control can simultaneously regulate both the rotor speed and the floating platform angle relative to horizontal [S4], [S69], [S70].

REFERENCES

- [S63] A. R. Henderson, C. Morgan, B. Smith, H. C. Sorenson, R. J. Barthelmie, and B. Boesmans, "Offshore wind energy in Europe—A review of the state-of-the-art," *Wind Energy*, vol. 6, no. 1, pp. 35–52, 2003.
- [S64] W. Musial and S. Butterfield. (2004). Future for offshore wind energy development in the United States. *Proc. Energy Ocean* [Online]. Available: <http://oce.uri.edu/oce495s1/2008/Musial%20et%20al%202004.pdf>
- [S65] J. Jonkman. (2007). Dynamics modeling and loads analysis of an offshore floating wind turbine, Ph.D. dissertation, Univ. Colorado at Boulder [Online]. Available: <http://www.nrel.gov/docs/fy08osti/41958.pdf>
- [S66] J. Jonkman and D. Matha. (2009). A quantitative comparison of the responses of three floating platform concepts. *Proc. European Offshore Wind Conf. Expo.*, Stockholm, Sweden [Online]. Available: <http://www.nrel.gov/docs/fy10osti/46726.pdf>
- [S67] J. Jonkman, "Dynamics of offshore floating wind turbines—Model development and verification," *Wind Energy*, vol. 12, no. 5, pp. 459–492, 2009.
- [S68] J. Jonkman and P. D. Sclavounos, "Development of fully coupled aeroelastic and hydrodynamic models for offshore wind turbines," in *Proc. AIAA/ASME Wind Energy Symp.*, Reno, NV, 2006, AIAA 2006-995.
- [S69] H. Namik, K. Stol, and J. Jonkman, "State-space control of tower motion for deepwater floating offshore wind turbines," in *Proc. AIAA/ASME Wind Energy Symp.*, Reno, NV, 2008, AIAA 2008-1307.
- [S70] H. Namik and K. Stol, "Individual blade pitch control of a floating offshore wind turbine on a tension leg platform," in *Proc. AIAA/ASME Wind Energy Symp.*, Orlando, FL, 2010, AIAA 2010-999.

PI gains on many utility-scale wind turbines are gain scheduled because the pitch authority is nonlinear in Region 3. The output signal can be either blade pitch angle or rate of change. A summary of Region 3 pitch control for speed regulation is provided in [33]. A systematic method for selecting the PID pitch control gains is presented in [34].

CART2 operational pitch angle data in Regions 2 and 3 is shown in Figure 16. The desired blade pitch angle changes from its nominal value only in Region 3, when it is used to limit rotor speed and power. The 600-kW CART2 has a maximum pitch rate of 18°/s, which is higher than the typical pitch rate on utility-scale turbines.

While collective blade pitch requires only a single-input, single-output (SISO) controller, many utility-scale turbines allow the blades to be pitched independently. If additional sensors and measurements, such as strain gauges measuring tower or blade bending moments, are available for feedback, then multi-input, multi-output (MIMO) individual blade pitch controllers can be designed for improved performance [35]–[37].

ISSUES IN WIND TURBINE CONTROL

The increasing dimensions of wind turbines lead to the increase in the loads on wind turbine structures. Because of increasing rotor size and spatially varying loads along the blade, individual blade pitch control can reduce the negative effects of sub-rotor-sized turbulent structures. Additional pitch control loops can be used to damp fore-aft tower motion or additional structural vibrations in Region 3.

Given the complexity of the wind turbine system, the stability of the complete plant plus control system cannot be proven. The multiple control loops interact, as do the multiple degrees of freedom of the turbine, especially as wind turbines become larger and have lower natural frequencies. A unified MIMO framework for individual blade pitch control can achieve significant load reduction for floating offshore wind turbines with strong coupling across degrees of freedom [35]–[38].

Because wind turbine control is often achieved using two distinct control loops for Regions 2 and 3, the transition between regions can be problematic. For some

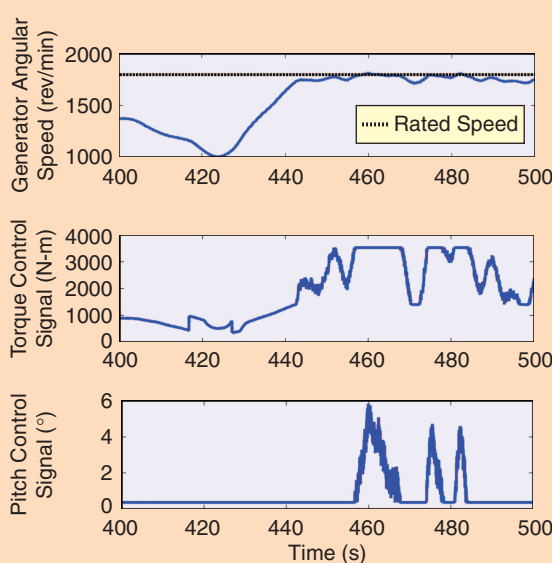


FIGURE 16 Experimental generator speed and torque and pitch control signals for CART2 in normal operation. The rated speed for CART2 is 1800 rev/min; when this rated value is reached, the torque control signal is saturated at its maximum value, and pitch control is used to limit turbine power.

turbines, the maximum structural damage occurs due to extreme and fatigue loads during this transition. Often, the act of switching between Region 2 and 3 controllers contributes to the problem.

The CART2 baseline controller, for example, uses an additional control region called Region 2.5 to facilitate switching between Region 2 and 3 control. The primary objective of the Region 2.5 control strategy, described in [37] and [39], is to connect Regions 2 and 3 controllers linearly in the generator torque versus generator speed plane. Unfortunately, this linear connection does not result in smooth transitions, and the discontinuous slopes in the torque control curve can contribute to excessive loading on the turbine. CART2 uses a saturation block on pitch angle in Region 2, and pitch control becomes active, that is, unsaturated, when rotor speed is greater than 99% of rated speed. A poor CART2 transition is shown in Figure 17.

Wind turbines can also be damaged when they are stopped as a result of supervisory control action due to high winds or fault conditions. However, little or no active control is performed when the turbine is stopped, although the yaw angle can be changed to accommodate changes in wind direction, which can prevent some damage.

In addition to the possibility of improving control when the turbine is stopped, advanced fault detection and turbine protection schemes are of interest to the wind industry. Stopping the turbine in the case of emergency, which might entail pitching the blades to a predetermined stop position at maximum pitch rate and setting the mechanical brakes with which the rotor is equipped, can also cause damage to the machine and must be done only when a turbine failure is suspected.

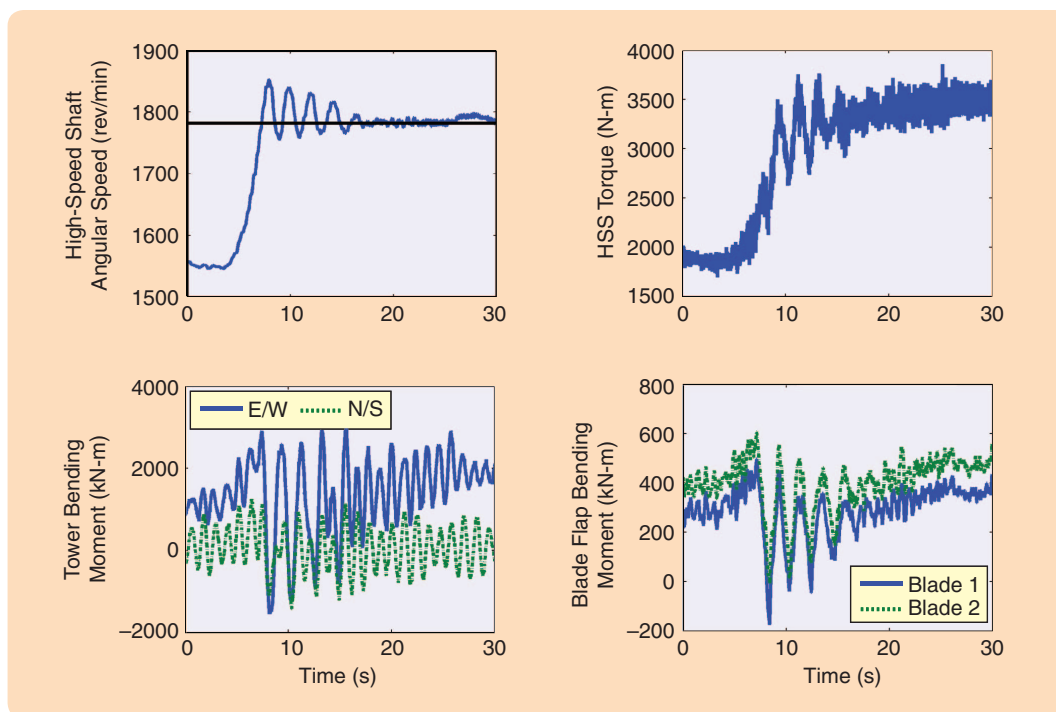


FIGURE 17 Experimental CART2 data during a poor transition from Region 2 to Region 3. E/W and N/S indicate tower bending directions in the east-west and north-south directions. The poor transition is partly caused by the lack of a smooth switching function.

Finally, controller performance depends on modeling accuracy. For instance, a realistic 5% modeling error in the optimal tip-speed ratio λ_* can cause an energy loss of around 1–3% in Region 2 [40]. This 1–3% can be a significant loss in this industry, with each 1% loss costing a 100-MW wind farm US\$123,000 per year by a conservative estimate. Even disregarding model errors, the dynamical behavior of a wind turbine changes over time due to wear, debris buildup on the blades, and environmental conditions. As such, adaptive methods can be used to tune controllers to improve performance compared to time-invariant methods [7], [32], [41]–[43].

While wind turbine dynamics can be modeled using first principles, efficient methods for obtaining models from measurements also exist, including the development of closed-loop identification methods for determining linear parameter-varying models [44]. These models can be used for robust control. Modeling of wind turbines and wind farms is further discussed in [29].

Further issues in wind turbine and wind farm control and current advanced control strategies are discussed in “Advanced Control of Wind Turbines,” “Modeling and Control of Wind Farms,” and “Offshore Wind Turbines.”

CONCLUSIONS

This tutorial describes the control of wind turbines and wind farms from a systems and control engineering point of view. In a walk around the wind turbine control loops, we discuss the goals of each loop and overview the typical actuation and sensing available on commercial turbines. We cover the modeling and control of individual wind turbines and outline several areas for further research, including MIMO control, combined feedforward and feedback control, coordinated control of arrays of wind turbines on wind farms, control of floating offshore wind turbines, and new sensing capabilities that can open up paradigms for advanced control approaches.

The rapidly growing wind energy industry has led to a large demand for better modeling and control of wind turbines and wind farms. The uncertainties and difficulties in measuring the wind inflow to wind turbines and wind farms makes the control challenging, and we recommend that more advanced modeling by means of system identification techniques and advanced control approaches be explored to reduce the cost of wind energy. By enabling this clean renewable energy source to provide and reliably meet the world’s electricity needs, we can help to meet the challenge of satisfying the world’s energy requirements in the future. Wind energy can be enabled by developing advanced wind turbine control systems. The application of advanced controls for wind energy systems is still in its youth, and various techniques such as iterative learning control, model predictive control, and H_∞ control have yet to be fully explored.

ACKNOWLEDGMENTS

The authors thank Jason Jonkman, Mari Shirazi, Florence Bocquet, Danny Abramovitch, Brian Rigney, Rod Frehlich,

Neil Kelley, Todd Murphey, and Fiona Dunne for reviewing and providing comments and suggestions on an earlier draft of this article. We also thank Danny Abramovitch for the idea of taking a “Walk Around the Loop” and Lee Jay Fingersh for many photos. The authors further gratefully acknowledge funding support from the U.S. National Renewable Energy Laboratory, the U.S. National Science Foundation, and industry for research in various aspects of control of wind turbines.

AUTHOR INFORMATION

Lucy Y. Pao (pao@colorado.edu) received the B.S., M.S., and Ph.D. in electrical engineering from Stanford University. Her interests are in the areas of control systems, multisensor data fusion, and haptic and multimodal visual-haptic-audio interfaces, with applications to wind turbines, power converters, tape systems, disk drives, atomic force microscopes, satellites, and scientific visualization. She is the Richard and Joy Dorf Professor of Electrical, Computer, and Energy Engineering at the University of Colorado at Boulder (CU-Boulder); a fellow of the Renewable and Sustainable Energy Institute, a joint institute between CU-Boulder and the National Renewable Energy Laboratory; and a member of the 2010–2011 U.S. Defense Science Study Group. She is also the scientific director for the Center for Research and Education in Wind (CREW), a multi-institutional wind energy center involving CU-Boulder, the National Renewable Energy Laboratory, Colorado School of Mines, and Colorado State University, in partnership with the National Oceanic and Atmospheric Administration and the National Center for Atmospheric Research. She can be contacted at the ECEE Department, UCB 425, University of Colorado, Boulder, CO 80309-0425 USA.

Kathryn E. Johnson received the B.S. in electrical engineering from Clarkson University in 2000 and the M.S. and Ph.D. in electrical engineering from the University of Colorado in 2002 and 2004, respectively. In 2005, she completed a postdoctoral research assignment studying adaptive control of variable-speed wind turbines at the National Renewable Energy Laboratory’s National Wind Technology Center. In October 2005, she was appointed the Clare Boothe Luce assistant professor at the Colorado School of Mines (CSM) in the Division of Engineering. Since 2007, she has also been the CSM Site Director for the Center for Research and Education in Wind (CREW). Her research interests are in control systems and control applications, specifically wind energy.

REFERENCES

- [1] World Wind Energy Association. (2010). World wind energy installed capacity [Online]. Available: <http://www.wwindea.org>
- [2] U.S. Department of Energy Office of Energy Efficiency and Renewable Energy. (2010). U.S. installed wind capacity and wind project locations [Online]. Available: http://www.windpoweringamerica.gov/wind_installed_capacity.asp
- [3] J. M. Roney. (2010). Wind power soared past 150,000 megawatts in 2009 [Online]. Available: http://www.earth-policy.org/index.php?/indicators/wind_power_2010

- [4] U.S. Department of Energy Office of Energy Efficiency and Renewable Energy. (2008). 20% wind energy by 2030 [Online]. Available: <http://www1.eere.energy.gov/windandhydro/pdfs/41869.pdf>
- [5] J. F. Manwell, J. G. McGowan, and A. L. Rogers, *Wind Energy Explained: Theory, Design, and Application*. West Sussex, England: Wiley, 2002.
- [6] T. Burton, D. Sharpe, N. Jenkins, and E. Bossanyi, *Wind Energy Handbook*. West Sussex, England: Wiley, 2001.
- [7] K. E. Johnson. (2004). Adaptive torque control of variable speed wind turbines, Ph.D. dissertation, Univ. Colorado at Boulder [Online]. Available: <http://www.nrel.gov/docs/fy04osti/36265.pdf>
- [8] A. Betz, *Introduction to the Theory of Flow Machines*. Oxford: Pergamon, 1966.
- [9] Danish Wind Industry Association. (2003). Turbines: How many blades [Online]. Available: <http://www.talentfactory.dk/en/tour/design/concepts.htm>
- [10] N. D. Kelley, B. J. Jonkman, and G. N. Scott. (2006). The great plains turbulence environment: Its origins, impact, and simulation. *Proc. AWEA's WindPower Conf.*, Pittsburgh, PA [Online]. Available: <http://www.nrel.gov/docs/fy07osti/40176.pdf>
- [11] M. Harris, M. Hand, and A. Wright. (2006). Lidar for turbine control, NREL, Golden, CO, NREL Tech. Rep. TP-500-39154 [Online]. Available: <http://www.nrel.gov/docs/fy06osti/39154.pdf>
- [12] M. Hand. (2003). Mitigation of wind turbine/vortex interaction using disturbance accommodating control, Ph.D. dissertation, Univ. Colorado at Boulder [Online]. Available: <http://www.nrel.gov/docs/fy04osti/35172.pdf>
- [13] N. D. Kelley, R. M. Osgood, J. T. Bialasiewicz, and A. Jakubowski, "Using wavelet analysis to assess turbulence/rotor interactions," *Wind Energy*, vol. 3, pp. 121–134, 2000.
- [14] R. Frehlich and N. D. Kelley, "Measurements of wind and turbulence profiles with scanning Doppler LIDAR for wind energy applications," *IEEE J. Select. Topics Appl. Earth Observations Remote Sens.*, vol. 1, no. 1, pp. 42–47, 2008.
- [15] T. Mikkelsen, K. Hansen, N. Angelou, M. Sjoholm, M. Harris, P. Hadley, R. Scullion, G. Ellis, and G. Vives, "LIDAR wind speed measurements from a rotating spinner," in *Proc. European Wind Energy Conf.*, Warsaw, Poland, 2010, pp. 1–8.
- [16] D. Schlipf, D. Trabucchi, O. Bischoff, M. Hofass, J. Mann, T. Mikkelsen, A. Rettenmeier, J. J. Trujillo, and M. Kuhn, "Testing of frozen turbulence hypothesis for wind turbine applications with a scanning LIDAR system," in *Proc. Int. Symp. Advancement of Boundary Layer Remote Sensing*, Paris, France, 2010, pp. 1–4.
- [17] M. Sjoholm, T. Mikkelsen, L. Kristensen, J. Mann, P. Kirkegaard, S. Kapp, D. Schlipf, and J. J. Trujillo, "Spectral analysis of wind turbulence measured by a Doppler LIDAR for velocity fine structure and coherence studies," in *Proc. Int. Symp. Advancement of Boundary Layer Remote Sensing*, Paris, France, 2010, pp. 1–4.
- [18] M. Hand and M. Balas, "Blade load mitigation control design for a wind turbine operating in the path of vortices," *Wind Energy*, vol. 10, pp. 339–355, 2007.
- [19] Y. Amirat, M. E. H. Benbouzid, E. Al-Ahmar, B. Bensaker, and S. Turri, "A brief status on condition monitoring and fault diagnosis in wind energy conversion systems," *Renewable Sustainable Energy Rev.*, vol. 13, pp. 2629–2636, 2009.
- [20] Z. Hameed, S. H. Ahn, and Y. M. Cho, "Practical aspects of a condition monitoring system for a wind turbine with emphasis on its design, system architecture, testing and installation," *Renewable Energy*, vol. 35, pp. 879–894, 2010.
- [21] K. E. Johnson, L. Fingersh, and A. Wright, "Controls advanced research turbine: Lessons learned during advanced controls testing," NREL, Golden, CO, NREL Tech. Rep. TP-500-38130, 2005.
- [22] F. D. Bianchi, H. De Battista, and R. J. Mantz, *Wind Turbine Control Systems: Principles, Modelling and Gain Scheduling Design*. New York: Springer-Verlag, 2006.
- [23] E. A. Bossanyi, *GH Bladed Theory Manual*, Garrad Hassan and Partners Ltd., Bristol, U.K., 2003.
- [24] J. Jonkman and M. Buhl, *FAST User's Guide*, NREL/EL-500-38230, Golden, CO, 2005.
- [25] B. Jonkman, *TurbSim User's Guide: Version 1.50*, NREL/EL-500-46198, Golden, CO, 2009.
- [26] T. J. Larsen and A. M. Hansen, *How 2 HAWC2, The User's Manual*, Risø-R-1597, Riso Nat. Lab. Tech. Univ. Denmark, Roskilde, Denmark, 2007.
- [27] P. Harris and P. Migliore, "Semi-empirical aeroacoustic noise prediction code for wind turbines," NREL, Golden, CO, NREL Tech. Rep. TP-500-34478, 2003.
- [28] P. Moriarty, "Safety factor calibration for wind turbine extreme loads," *Wind Energy*, vol. 11, no. 6, pp. 601–612, 2008.
- [29] P. Moriarty and C. P. Butterfield, "Wind turbine modeling overview for control engineers," in *Proc. American Control Conf.*, St. Louis, MO, 2009, pp. 2090–2095.
- [30] S. Oye, "Simulations of loads on a wind turbine including turbulence," in *Proc. IEA Meeting*, Stockholm, Sweden, 1991, pp. 99–105.
- [31] MSC Software Corporation. (2011). Adams multibody dynamics software [Online]. Available: <http://www.mscsoftware.com/Products/CAE-Tools/Adams.aspx>
- [32] K. E. Johnson, L. Y. Pao, M. J. Balas, and L. J. Fingersh, "Control of variable-speed wind turbines: Standard and adaptive techniques for maximizing energy capture," *IEEE Control Syst. Mag.*, vol. 26, no. 3, pp. 70–81, June 2006.
- [33] K. Stol and M. J. Balas, "Periodic disturbance accommodating control for speed regulation of wind turbines," in *Proc. AIAA/ASME Wind Energy Symp.*, Reno, NV, 2002, pp. 310–320.
- [34] M. M. Hand and M. J. Balas, "Systematic controller design methodology for variable-speed wind turbines," *Wind Eng.*, vol. 24, no. 3, pp. 169–187, 2000.
- [35] F. Lescher, J. Y. Zhao, and A. Martinez. (2006). Multiobjective control of a pitch regulated wind turbine for mechanical load reduction. *Proc. Int. Conf. Renewable Energy and Power Quality*, Granada, Spain [Online]. Available: <http://www.icrepq.com/papers-icrepq06.htm>
- [36] M. Geyler and P. Caselitz, "Robust multivariable pitch control design for load reduction on large wind turbines," *J. Solar Energy Eng.*, vol. 130, no. 3, pp. 031014-1–031014-12, 2008.
- [37] J. H. Laks, L. Y. Pao, and A. Wright, "Control of wind turbines: Past, present, and future," in *Proc. American Control Conf.*, St. Louis, MO, 2009, pp. 2096–2103.
- [38] J. H. Laks, L. Y. Pao, A. Wright, N. Kelley, and B. Jonkman, "Blade pitch control with preview wind measurements," in *Proc. AIAA/ASME Wind Energy Symp.*, Orlando, FL, 2010, AIAA 2010-251.
- [39] L. Fingersh and K. Johnson, "Baseline results and future plans for the NREL controls advanced research turbine," in *Proc. AIAA/ASME Wind Energy Symp.*, Reno, NV, 2004, pp. 87–93.
- [40] L. Fingersh and P. Carlin, "Results from the NREL variable-speed test bed," in *Proc. AIAA/ASME Wind Energy Symp.*, Reno, NV, 1998, pp. 233–237.
- [41] J. Freeman and M. Balas, "An investigation of variable speed horizontal-axis wind turbines using direct model-reference adaptive control," in *Proc. AIAA/ASME Wind Energy Symp.*, Reno, NV, 1999, pp. 66–76.
- [42] S. A. Frost, M. J. Balas, and A. D. Wright, "Direct adaptive control of a utility-scale wind turbine for speed regulation," *Int. J. Robust Nonlinear Control (Special Issue: Wind Turbines, New Challenges and Advanced Control Solutions)*, vol. 19, no. 1, pp. 59–71, 2009.
- [43] Y. D. Song, B. Dhinakaran, and X. Bao, "Variable speed control of wind turbines using nonlinear and adaptive algorithms," *J. Wind Eng. Ind. Aerodyn.*, vol. 85, pp. 293–308, 2000.
- [44] J. W. van Wingerden, I. Houtzager, F. Felici, and M. Verhaegen, "Closed-loop identification of the time-varying dynamics of variable-speed wind turbines," *Int. J. Robust Nonlinear Control*, vol. 19, no. 1, pp. 4–21, 2009.
- [45] A. M. L. Johnsen. (2011). Wind power [Online]. Available: <http://www.renewableenergy.no>
- [46] Aerospaceweb.org. (2010). Boeing 747 long-range jetliner [Online]. Available: <http://www.aerospaceweb.org/aircraft/jetliner/b747>
- [47] Steinninn. (2011). American football [Online]. Available: http://en.wikipedia.org/wiki/American_football
- [48] Symscape: Computational fluid dynamics for all. (2007). Darrieus vertical-axis wind turbine [Online]. Available: <http://www.symscape.com/node/406>
- [49] U.S. Department of Energy. (2010). Energy efficiency and renewable energy [Online]. Available: http://www1.eere.energy.gov/windandhydro/wind_low.html
- [50] R. Banta, Y. Pichugina, N. Kelley, B. Jonkman, and W. Brewer, "Doppler lidar measurements of the Great Plains low-level jet: Applications to wind energy," in *Proc. 14th Int. Symp. Advancement of Boundary Layer Remote Sensing*, 2008, pp. 1–5.

